Polarization anisotropy in GaN films for different nonpolar orientations studied by polarized photoreflectance spectroscopy

Pranob Misra, Udo Behn,[a] Oliver Brandt, and Holger T. Grahn[b]
Paul-Drude-Institut für Festkörperelektronik, Hausvogteiplatz 5-7, 10117 Berlin, Germany

Bilge Imer, Shuji Nakamura, Steven P. DenBaars, and James S. Speck
Materials Department and ERATO/JST UCSB Group, University of California, Santa Barbara, California 93106-5050

(Received 3 March 2006; accepted 12 March 2006; published online 21 April 2006)

We use photoreflectance (PR) spectroscopy to study the electronic band structure modification of GaN films grown along different nonpolar orientations due to biaxial, anisotropic in-plane strain. The exciton transition energies of an unstrained, high-quality *C*-plane GaN film are used to accurately determine the crystal-field and spin-orbit splitting energies. For films with a nonpolar orientation, the resonant features observed in the PR spectra exhibit a strong in-plane polarization anisotropy and different transition energies from the ones measured in the *C*-plane GaN film. The deformation potential D_5 is accurately determined from four GaN films with a nonpolar orientation using the measured energies together with the polarization properties and out-of-plane strain.
 [DOI: 10.1063/1.2198086]

The electrical and optical properties of semiconductors are mainly governed by the electronic band structure (EBS) in the vicinity of the absolute valence-band maximum and conduction-band minimum. In heteroepitaxial layers, the EBS of the film material can be strongly modified because of the strain, which is present due to the mismatch of the lattice constants as well as the thermal expansion coefficients between the film and substrate. To correctly predict the optical transition energies and polarization properties of the strained film, it is important to determine the dependence of the EBS modification on in-plane strain. For the wurtzite crystal structure, the strain-induced EBS modification in the vicinity of the Γ point can be theoretically estimated by adopting the $\mathbf{k}\cdot\mathbf{p}$ perturbation approach outlined by Bir and Pikus.[1] Since we are only interested in the transition energies at the Γ point, the number of required parameters in the $\mathbf{k}\cdot\mathbf{p}$ perturbation approach is reduced to the crystal-field (Δ_{cr}) and spin-orbit (Δ_{so}) splitting energies and six distinct deformation potentials D_1–D_6.

For materials with the wurtzite crystal structure, Δ_{cr} and Δ_{so} are usually deduced from the differences of the *A*-, *B*-, and *C*-exciton transition energies (for strained samples we will use the notation T_1, T_2, and T_3 in order of increasing energy), while the deformation potentials are determined from strain-dependent measurements. For GaN, a large number of values for Δ_{cr}, Δ_{so}, and D_5, are reported in the literature, which are derived from both first principle calculations and experimental data.[2–5] The exciton transition energies, which are used to obtain Δ_{cr}, Δ_{so}, and D_5, can vary significantly from sample to sample because of the residual strain in the films, which depends on the film thickness, the growth technique, and the respective substrate. For optical spectra of GaN layers, the average strain mainly determines the energies of the excitonic transitions, while the crystal quality and built-in strain mainly influences the width and shape of the excitonic features through the inhomogeneous contribution to the strain distribution.

To improve the accuracy of Δ_{cr}, Δ_{so}, and D_5, we have first investigated the optical properties of a high-quality, unstrained *C*-plane GaN layer grown on bulk GaN near the fundamental band gap to determine the exciton transition energies, which are directly related to Δ_{cr} and Δ_{so}. Second, we use photoreflectance (PR) spectroscopy to study the EBS modification of *M*- and *A*-plane GaN films for different in-plane strain values. The experimentally observed transition energies and polarization properties of four different samples are compared with the calculated ones using the $\mathbf{k}\cdot\mathbf{p}$ perturbation approach with the improved values for Δ_{cr} and Δ_{so}. In this way, we obtain a more accurate estimate of the deformation potential D_5.

A 1-μm-thick *C*-plane GaN film (sample I) was grown by plasma-assisted molecular-beam epitaxy (PAMBE) on a commercially available 200-μm-thick GaN template. In addition, we investigated four samples with a nonpolar orientation including a 1.22-μm-thick (sample II) and a 0.7-μm-thick *M*-plane GaN film (sample III) also grown by PAMBE on γ-$LiAlO_2(100)$ substrates.[6,7] High-resolution triple-axis x-ray diffraction (XRD) measurements performed at 295 K reveal that sample I is unstrained ($\Delta a/a < 10^{-4}$), while sample II (III) has an out-of-plane dilation $\epsilon_{yy}=0.29\%$ (0.42%) with *x*, *y*, and *z* being parallel to the $[11\bar{2}0]$, $[1\bar{1}00]$, and [0001] directions, respectively. The *A*-plane GaN films consist of a 0.2-μm-thick AlN nucleation layer followed by a 1-μm-thick, undoped GaN film grown by metal-organic vapor-phase epitaxy (MOVPE) on *A*-plane SiC (sample IV) and *R*-plane sapphire (sample V). XRD measurements demonstrate that sample IV (V) has an out-of-plane dilation $\epsilon_{xx}=0.04\%$ (0.09%). A detailed description of the growth conditions and the postgrowth characterization of the MOVPE films can be found in Refs. 8 and 9.

The reflectance and PR measurements were carried out at near normal incidence between 6 and 10 K. For the PR measurements, the pump beam at 300 nm (4.13 eV) was obtained from a combination of a 150 W Xe lamp with a 1 m monochromator, while the beam for both the reflectance and

[a]Permanent address: Fachhochschule Schmalkalden, Blechhammer 4 und 9, 98574 Schmalkalden, Germany.
[b]Electronic mail: htgrahn@pdi-berlin.de

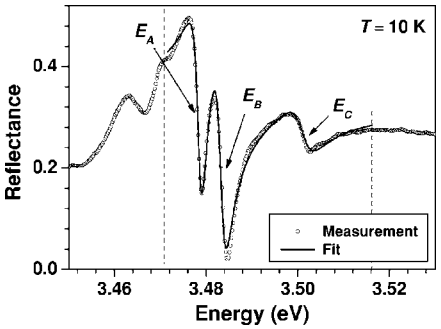

FIG. 1. Reflectance spectrum (circles) of sample I measured at 10 K. The solid line indicates a fit to Eq. (1) for the energy range marked by the vertical dashed lines resulting in E_A=3.478, E_B=3.483, and E_C=3.501 eV.

PR probe was derived by dispersing the light from a 75 W Xe lamp with a 0.64 m monochromator and polarizing it with a Glan-Taylor prism. The reflected light was detected by a silicon photodiode using standard lock-in techniques.

The reflectance spectrum for sample I at 10 K is shown in Fig. 1. It exhibits very sharp resonances due to the free *A*, *B*, and *C* excitons. The reflectance spectrum is fitted with a Lorentzian line shape[10]

$$R(E) = R_0 + R_X \Re\mathrm{e}\left[\frac{E_X - E + i\Gamma_X}{\Gamma_X^2 + (E - E_X)^2} e^{i\Theta_X}\right], \tag{1}$$

where X denotes the exciton A, B, or C, $\Re\mathrm{e}$ the real part of the function, R_X the reflectance, E_X the corresponding transition energy, and Γ_X a broadening parameter. Θ_X is a phase factor, which accounts for the mixture of the real and imaginary components of the dielectric function as well as the influence of nonuniform electric fields, while R_0 corresponds to the background. The transition energies obtained for sample I are E_A=3.478, E_B=3.483, and E_C=3.501 eV. These values agree well with corresponding exciton transition energies measured for unstrained films grown on GaN substrates.[11–13]

To determine Δ_{cr} and Δ_{so} from the exciton transition energies for unstrained *C*-plane GaN film, we apply Hopfield's quasicubic model developed for the wurtzite crystal structure.[14] The relation between the differences $\delta_{X,Y} = E_X - E_Y$ in the exciton transition energies and the splitting energies is given using $\delta_+ = \delta_{C,A}$ and $\delta_- = \delta_{B,A}$ by

$$\delta_\pm = \frac{\Delta_{\mathrm{cr}} + \Delta_{\mathrm{so}}}{2} \pm \sqrt{\left(\frac{\Delta_{\mathrm{cr}} + \Delta_{\mathrm{so}}}{2}\right)^2 - \frac{2}{3}\Delta_{\mathrm{cr}}\Delta_{\mathrm{so}}}. \tag{2}$$

Solving the above equations for $\Delta_- = \Delta_{\mathrm{cr}}$ and $\Delta_+ = \Delta_{\mathrm{so}}$ leads to

$$\Delta_\pm = \tfrac{1}{2}(\delta_{C,A} + \delta_{B,A} \pm \sqrt{2\delta_{C,B}^2 - \delta_{B,A}^2 - \delta_{C,A}^2}). \tag{3}$$

Using the values for E_X given above, we obtain Δ_{cr} =9.2 meV and Δ_{so}=18.9 meV. While the spin-orbit splitting energy is in good agreement with values in the literature, there is a wide variation in the values obtained for the crystal-field splitting energy, since this energy is more strongly affected by strain.[5] However, our value for Δ_{cr} is in very good agreement with the one given by Stępniewski *et al.*,[11] which was also obtained for homoepitaxial GaN.

Figures 2(a)–2(c) display the PR spectra for samples III, IV, and V, respectively, measured at 10 K for light linearly polarized parallel ($\boldsymbol{E}\|\boldsymbol{c}$) or perpendicular ($\boldsymbol{E}\perp\boldsymbol{c}$) to the *c* axis in the film plane. In addition to the *z* axis, the *x* axis (*y* axis) lies also in the film plane for *M* plane (*A*-plane) GaN

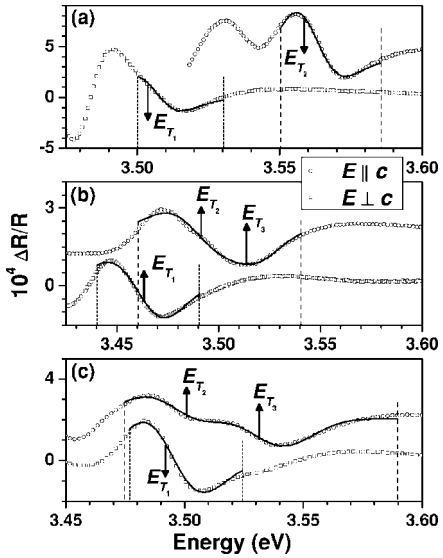

FIG. 2. Photoreflectance spectra of (a) sample III, (b) sample IV, and (c) sample V measured for light polarizations $\boldsymbol{E}\|\boldsymbol{c}$ (circles) and $\boldsymbol{E}\perp\boldsymbol{c}$ (squares) at 10 K. The solid lines indicate the fits described in the text for the energy ranges marked by the vertical dashed lines. The resulting energies for the T_1, T_2, and T_3 transitions are marked by E_{T_1}, E_{T_2}, and E_{T_3}, respectively, and listed in Table I. For clarity, the PR spectra for $\boldsymbol{E}\|\boldsymbol{c}$ in (a) are shifted vertically by 4×10^{-4}, while the shift in (b) and (c) is 2×10^{-4}.

films. The PR spectra have a complex line shape, which is dominated by excitonic features. However, on the low-energy and high-energy sides of the PR spectra, these features are superimposed by interference fringes and Franz-Keldysh oscillations, respectively. To extract the exciton transition energies from the PR spectra, we use the first derivative of a Gaussian oscillator and exclude the regions of interference fringes and Franz-Keldysh oscillations for the fit. For sample III, the PR spectra in Fig. 2(a) reveal a single transition at 3.504 eV for $\boldsymbol{E}\perp\boldsymbol{c}$, while another transition appears at 3.558 eV for $\boldsymbol{E}\|\boldsymbol{c}$. For sample IV, the situation is altogether different. Here the measurements shown in Fig. 2(b) suggest a single transition at 3.463 eV for $\boldsymbol{E}\perp\boldsymbol{c}$ and two transitions at 3.493 and 3.514 eV for $\boldsymbol{E}\|\boldsymbol{c}$. For sample V, the measurements shown in Fig. 2(c) reveal that there is a single transition at 3.493 eV for $\boldsymbol{E}\perp\boldsymbol{c}$ and two transitions at 3.499 and 3.531 eV for $\boldsymbol{E}\|\boldsymbol{c}$. All experimental values for the transition energies and out-of-plane dilation of samples III–V are listed in Table I. In addition, the values for sample II taken from Ref. 4 are also included.

A systematic approach to accurately determine the deformation potential D_5 is the reproduction of the transition energies and polarization properties of the resonant features observed in the PR spectra for all four films with a nonpolar orientation listed in Table I using the $\mathbf{k}\cdot\mathbf{p}$ perturbation approach presented in Ref. 4 with a single set of parameters. We vary the deformation potential D_5 over a range of values and find that D_5=−3.6 eV results in the best agreement of the measured and calculated transition energies taking into account the oscillator strengths and the out-of-plane strain. All parameters except Δ_{cr}, Δ_{so}, and D_5 are taken from Ghosh *et al.*[4] The resulting transitions energies and relative oscillator strengths f_β, where $\beta = x$, y, and z, are compiled in Table I. A value of 1 for the oscillator strength corresponds to a completely linearly polarized transition.

For sample II, the transition energies calculated for the strain values of ϵ_{xx}=−0.73% and ϵ_{zz}=−0.22% agree very well with the measured ones. The calculated oscillator

TABLE I. Measured (E_{expt}) and calculated energies (E_{cal}) of the transitions T_i (i=1, 2, and 3) for samples II, III, IV, and V grown on substrate S with a thickness d for $\boldsymbol{E}\perp\boldsymbol{c}$ ($\perp$) and $\boldsymbol{E}\|\boldsymbol{c}$ ($\|$), measured out-of-plane dilation ϵ_{opd}, in- and out-of-plane strain values $\epsilon_{\beta\beta}$ obtained from the calculated transition energies, and calculated oscillator strengths f_β with β=x, y, or z for the corresponding linear polarization. For the calculations, we used the parameters Δ_{cr} =9.2 meV, Δ_{so}=18.9 meV, and D_5=−3.6 eV. The experimental values for sample II were taken from Ref. 4.

		Experiment		**k·p** calculations					
Sample	S d (μm)	E_{expt} (eV)	ϵ_{opd}	$\epsilon_{\beta\beta}$	T_i	E_{cal} (eV)	f_x	f_y	f_z
II	$LiAlO_2$	3.498 ($\perp$)		ϵ_{xx}=−0.73%	T_1	3.498	**0.98**	0.00	0.02
(M)	1.22	3.546 ($\|$)		ϵ_{zz}=−0.22%	T_2	3.544	0.01	0.05	**0.94**
			ϵ_{yy}=0.29%	ϵ_{yy}=0.33%	T_3	3.578	0.01	**0.95**	0.04
III	$LiAlO_2$	3.504 ($\perp$)		ϵ_{xx}=−0.91%	T_1	3.504	**0.98**	0.01	0.01
(M)	0.7	3.558 ($\|$)		ϵ_{zz}=−0.30%	T_2	3.557	0.01	0.02	**0.97**
			ϵ_{yy}=0.42%	ϵ_{yy}=0.42%	T_3	3.602	0.01	**0.97**	0.02
IV	SiC	3.463 ($\perp$)		ϵ_{yy}=−0.29%	T_1	3.463	0.04	**0.95**	0.01
(A)	1.0	3.493 ($\|$)		ϵ_{zz}=0.21%	T_2	3.489	0.89	0.03	**0.08**
		3.514 ($\|$)	ϵ_{xx}=0.04%	ϵ_{xx}=0.05%	T_3	3.517	0.07	0.02	**0.91**
V	Al_2O_3	3.493 ($\perp$)		ϵ_{yy}=−0.17%	T_1	3.492	0.03	**0.85**	0.12
(A)	1.0	3.499 ($\|$)		ϵ_{zz}=−0.14%	T_2	3.503	0.30	0.04	**0.66**
		3.531 ($\|$)	ϵ_{xx}=0.09%	ϵ_{xx}=0.10%	T_3	3.521	0.67	0.11	**0.22**

strength of f_x=0.98 (f_z=0.94) suggests that the T_1 (T_2) transition is almost completely x polarized (z polarized). Because of the smaller thickness of sample III in comparison to sample II, ϵ_{yy} in sample III is significantly larger than in sample II (cf. Table I). The calculated and measured transition energies are in excellent agreement for ϵ_{xx}=−0.91% and ϵ_{zz}=−0.30% (comparable to the lattice mismatch between the film and substrate along the c axis), revealing that sample III has a larger biaxial, anisotropic in-plane strain than sample II. As expected, the transition energies of sample III are shifted to higher values due to the larger compressive strain. As for sample II, the calculated oscillator strength f_x =0.98 (f_z=0.97) of sample III suggests that the T_1 (T_2) transition is completely x polarized (z polarized). The transition between the conduction band and the third highest valence band, which gives rise to the T_3 transition, is y polarized for samples II and III. Under normal incidence, this transition is not accessible for M-plane films.

The polarization properties of samples IV and V are quite different from the ones of samples II and III, because the in-plane strain in the former samples is considerably smaller than in the latter ones. In samples IV and V, two transitions appear for $\boldsymbol{E}\|\boldsymbol{c}$ in contrast to samples II and III, while one transition is again measured for $\boldsymbol{E}\perp\boldsymbol{c}$. The calculated energies agree with the measured ones within the experimental accuracy of about 5 meV. According to the calculated oscillator strengths, the single transition for $\boldsymbol{E}\perp\boldsymbol{c}$ is almost completely y polarized (note the different in-plane axes because of the A-plane orientation), while the two transitions observed for $\boldsymbol{E}\|\boldsymbol{c}$ are due to a significant oscillator strength of the transitions T_2 and T_3 for z polarization. Note, however, that for sample IV f_z for T_2 is still rather small, which needs further investigation. The resulting in-plane strain values for sample IV (V) are ϵ_{yy}=−0.29% (−0.17%) and ϵ_{zz}=0.21% (−0.14%).

In conclusion, we have accurately determined the values for the crystal-field (9.2 meV) and spin-orbit splitting energies (18.9 meV) from the differences in the exciton transition energies of an unstrained C-plane GaN film. Using polarized PR spectroscopy, we have measured the exciton transition energies and polarization properties for several GaN films grown along different nonpolar orientations exhibiting different in-plane strain values. The improved values for the splitting energies are used to calculate the EBS modification due to strain. The comparison of the calculated transitions energies, oscillator strengths, and out-of-plane strain with the experimental results of four different samples leads to a deformation potential D_5=−3.6 eV.

The authors would like to thank Sandip Ghosh for his numerous invaluable contributions to this work.

[1] G. L. Bir and G. E. Pikus, *Symmetry and Strain-Induced Effects in Semiconductors* (Wiley, New York, 1974).
[2] M. Suzuki, T. Uenoyama, and A. Yanase, Phys. Rev. B **52**, 8132 (1995).
[3] W. Shan, R. J. Hauenstein, A. J. Fischer, J. J. Song, W. G. Perry, M. D. Bremser, R. F. Davis, and B. Goldenberg, Phys. Rev. B **54**, 13460 (1996).
[4] S. Ghosh, P. Waltereit, O. Brandt, H. T. Grahn, and K. H. Ploog, Phys. Rev. B **65**, 075202 (2002).
[5] I. Vurgaftman and J. R. Meyer, J. Appl. Phys. **94**, 3675 (2003).
[6] P. Waltereit, O. Brandt, M. Ramsteiner, R. Uecker, P. Reiche, and K. H. Ploog, J. Cryst. Growth **218**, 143 (2000).
[7] Y. J. Sun, O. Brandt, and K. H. Ploog, J. Vac. Sci. Technol. B **21**, 1350 (2003).
[8] M. D. Craven, S. H. Lim, F. Wu, J. S. Speck, and S. P. DenBaars, Appl. Phys. Lett. **81**, 469 (2002).
[9] M. D. Craven, F. Wu, A. Chakraborty, B. Imer, U. K. Mishra, S. P. DenBaars, and J. S. Speck, Appl. Phys. Lett. **84**, 1281 (2004).
[10] K. P. Korona, A. Wysmołek, K. Pakuła, R. Stępniewski, J. M. Baranowski, I. Grzegory, B. Łucznik, M. Wróblewski, and S. Porowski, Appl. Phys. Lett. **69**, 788 (1996).
[11] R. Stępniewski, K. P. Korona, A. Wysmołek, J. M. Baranowski, K. Pakuła, M. Potemski, G. Martinez, I. Grzegory, and S. Porowski, Phys. Rev. B **56**, 15151 (1997).
[12] M. Mayer, A. Pelzmann, M. Kamp, K. J. Ebeling, H. Teisseyre, G. Nowak, M. Leszczyński, I. Grzegory, S. Porowski, and G. Karczewski, Jpn. J. Appl. Phys., Part 2 **36**, L1634 (1997).
[13] K. Kornitzer, T. Ebner, K. Thonke, R. Sauer, C. Kirchner, V. Schwegler, M. Kamp, M. Leszczynski, I. Grzegory, and S. Porowski, Phys. Rev. B **60**, 1471 (1999).
[14] J. J. Hopfield, J. Phys. Chem. Solids **15**, 97 (1960).